Published in final edited form as:
Dalton Trans. 2013 June 14; 42(22): 8066–8069. doi:10.1039/c3dt50194a.

A europium(III)-based PARACEST agent for sensing singlet oxygen by MRI

Bo Song[a,d], **Yunkou Wu**[b], **Mengxiao Yu**[a], **Piyu Zhao**[a], **Cheng Zhou**[a], **Garry E. Kiefer**[a,c], and **A. Dean Sherry**[a,b]

A. Dean Sherry: sherry@utdallas.edu

[a]Department of Chemistry, University of Texas at Dallas, 800 West Campbell Road, Richardson, TX 75080, United States.. Fax: +1972-883-2907; Tel: +1972-883-2907

[b]Advanced Imaging Research Center, University of Texas Southwestern Medical Center, 5323 Harry Hines Boulevard, Dallas, TX75390, United States

[c]Macrocyclics, Inc., 1309 Record Crossing, Dallas, TX 75235, United States

[d]State Key Laboratory of Fine Chemicals, School of Chemistry, Dalian University of Technology, Dalian 116024, China

Abstract

A europium (III) DOTA-tetraamide complex was designed as a MRI sensor of singlet oxygen ($^1O_2$). The water soluble, thermodynamically stable complex reacts rapidly with $^1O_2$ to form an endoperoxide derivative that results in an ~3 ppm shift in the position of the Eu(III)-bound water chemical exchange saturation transfer (CEST) peak. The potential of using this probe to detect accumulation of the endoperoxide derivative in biological media by ratiometric CEST imaging was demonstrated.

Singlet oxygen ($^1O_2$), the lowest excited electronic state of molecular oxygen, is a highly unstable reactive oxygen species (ROS) that plays a significant role in many chemical and biological processes including cell signaling transduction and in host defense against intruding microorganisms.[1, 2] Singlet oxygen can also oxidize a variety of biological molecules including proteins, DNA and lipids resulting in inhibition of normal cell functions related to cancer, cardiovascular diseases and the aging process.[3-5] Moreover, artificial photochemical generation of $^1O_2$ is thought to be the primary species involved in destruction of malignant cells or tissues during photodynamic therapy (PDT).[6, 7] However, some aspects of PDT remain controversial partly due to the lack of a reliable detection method for $^1O_2$ *in vivo*.

Various methods for detection of $^1O_2$ have been reported. $^1O_2$ phosphorescence can be observed at 1270 nm[8, 9] but the phosphorescence efficiency is low and unsuitable for monitoring $^1O_2$ under physiological conditions because the $^1O_2$ lifetime is very short.[10] Consequently, other methods have been developed with improved sensitivity including electron spin resonance (ESR),[11] absorbance,[12] fluorescence [13, 14] and chemiluminescence (CL).[15] Unfortunately, these methods are not widely applicable *in vivo*.

Correspondence to: A. Dean Sherry, sherry@utdallas.edu.

†Electronic Supplementary Information (ESI) available: [Synthetic procedure, experimental detail, UV-VIS spectra, ^1H NMR Spectra, HPLC chromatograms, fluorescence spectra, CEST spectra as a function of applied B1, and CEST fitting data]. See DOI: 10.1039/b000000x/

Magnetic resonance imaging (MRI) is one of the most widely used, noninvasive diagnostic imaging tools in clinical medicine today. Exogenous contrast agents derived from paramagnetic metal complexes are often used to shorten the relaxation time of water protons to enhance tissue contrast in MRI. Over the past decade, a new type of MRI agent based on chemical exchange saturation transfer (CEST) offers an option to conventional Gd^{3+}-based T_1 agents as a platform for creating MR responsive sensors.[16, 17] It has been demonstrated that lanthanide complexes with various 1,4,7,10,-tetraazacyclo dodecane-1,4,7,10-tetraacetic acid (DOTA) tetraamide derivatives are quite versatile for creating responsive CEST agents. Eu^{3+} complexes with various DOTA-tetraamide ligands display an adequately slow water exchange rate to meet slow-to-intermediate exchange condition ($k_{ex} \leq \Delta\omega$) required for CEST. Moreover, the Eu^{3+}-water exchange peak is paramagnetically shifted well downfield of the bulk water resonance making selective activation of this exchange peak relatively convenient by MRI. Numerous studies have shown that the water CEST signal in various EuDOTA-tetraamide complexes is extremely sensitive to the chemical features of the coordinating amide side arms.[17, 18] Given these prior observations, we envisioned a new type of complex, EuL (Scheme 1), that might be used as CEST probe for $^1O_2$, wherein a 9-anthryl group is used as a specific reactive center for $^1O_2$.[13] The advantages of using a non-equilibrium probe design such as this for detection of short-lived, low concentration species such as $^1O_2$ was recently demonstrated by Liu, *et al*,[19] in a similar paraCEST system designed to detect NO. Our hypothesis in this work was that oxidation of the anthryl moiety to the irreversible, stable endoperoxide by reaction with $^1O_2$ would convert sufficient EuL to EP-EuL over time to allow detection by CEST imaging.

The ligand was synthesized in five-steps as outlined in Scheme S1 (supporting information). The corresponding endoperoxide was prepared by reacting EuL with chemically generated $^1O_2$ using MoO_4^{2-}/H_2O_2.[20] Production of EP-EuL was confirmed by UV-VIS, ^1H NMR, HPLC and mass spectra (Figure S1-S3). The absorption spectrum of EuL displayed two bands between 350–400 nm characterstic of the 9-anthryl moiety which disappeared after the formation of EP-EuL. The ^1H NMR spectra of EuL and EP-EuL in D_2O showed multiple resonances between 25-30 ppm characteristic of the four H_4 macrocyclic protons in Eu^{3+} complexes that exist in solution in a square-antiprism (SAP) coordination geometry.[21] The CEST signal of EuL showed a typical Eu^{3+}-water exchange peak near 50 ppm, again characteristic of a SAP isomer, that shifted to 53 ppm upon formation EP-EuL (Figure 1A). The bound water lifetimes (τ_M) of EuL and EP-EuL were determined by fitting the experimental CEST spectra to the Bloch equations modified for exchange.[22] This fitting procedure gave values of τ_M = 90 μs for EuL and 137 μs for EP-EuL at 298K, consistent with the sharper water exchange peak and slower water exchange rate in EP-EuL with more electron-withdrawing anthryl endoperoxide functionality.[18] The ~3 ppm frequency difference between the water exchange peaks in the complexes offered the possibility of imaging singlet oxygen as it accumulates (EuL → EP-EuL) using ratiometric methods. The CEST ratio of water intensities after presaturation at 54 *vs* 47 ppm was linear with $^1O_2$ concentration over a wide range (Figure 1B). Compared with intensity-based measurements, ratiometric detection provides a built-in correction for environmental effects and increases the selectivity and sensitivity of the measurement. Although the bound water lifetimes in EuL and EP-EuL were considerably shorter as expected at 310K (30 μs for EuL and 35 μs for EP-EuL), the ratio of CEST intensities *vs* $^1O_2$ concentration remained linear at the physiological temperature (figure S5).

Experiments were also peformed to detect singlet oxygen being produced by the irradiation of the water-soluble cationic porphyrin, TMPyP, an efficient $^1O_2$ photosensitizer often used in the context of photodynamic therapy.[7] As seen in Figure 1C, the CEST ratio (54/47) increased linearly with irradiation time up to 2 hours only in samples containing the

photosensitizer. On the basis of calibration curve shown in Figure 1B, one can conclude that ~80 percent of EuL was converted to EP-EuL after 2 hours of light irradiation.

To investigate the reaction specificity of EuL with $^1O_2$, the probe was exposed to a variety of other reactive oxygen species in aqueous buffer. No significant change in CEST signal was observed after exposure of EuL to $ONOO^-$, H_2O_2, •OH or $O_2^{-\bullet}$ (Figure 2A). Furthermore, in the presence of excess azide, a quencher of $^1O_2$,[14] the CEST signal of EuL was also unchanged. These results indicate that EuL is highly specific for $^1O_2$. The reaction rate of EuL with $^1O_2$ in an aqueous buffer was determined by use of an established method (Figure S6). [14] The reaction rate constant of EuL with $^1O_2$ was 4.9×10^8 M^{-1} s^{-1}, similar to the reaction rate constant of derivatives of anthrancene with $^1O_2$.[13] As an initial test of stablility, 5 mM EuL was mixed with 25 mM EDTA in Tris-HCl buffer, pH 7 and the sample was stirred for 4 hours at 298K. NMR analysis of the resulting mixture yielded a conditional stability constant of ~10^{20} for EuL by using the method described by Werts, *et al.*[23] The CEST signal of EuL was pH dependent below 4 and above pH 8 but relatively constant near physiological pH values (Figure S7). These combined results indicate that EuL may prove useful as a MRI sensor of $^1O_2$ in many chemical and biological environments.

As an initial test for probe toxicity, HeLa cells grown in tissue culture plates were incubated with 15 mM EuL in physiological saline for 1 hr in a 95/5% air/CO_2 chamber at 37°C, washed with PBS (5×) and harvested by treatment with trypsin. Cell viability, defined as the ratio of viable cells to total number of cells, was determined by trypan blue staining using a Neubauer hemacytometer. The cells showed no evidence of necrosis and > 97% of the cells were viable. Given that EuL is highly fluorescent as a result of strong emission from the anthryl group (385-455 nm, Figure S8), cell uptake of EuL was further examined by fluorescence microscopy. HeLa cells grown in glass cell culture dishes were incubated with 5 mM EuL in MEM for 1 h at 37°C in a 95% O_2/ 5% CO_2 chamber then washed five times with PBS and examined using a fluorescence microscope. As shown in Figures 2C and 2D, EuL appears to permeate the cell membrane and distribute throughout the cytoplasm. In separate experiments, HeLa cells cultured in a 75 cm^3 culture flask were loaded with 15 mM EuL for 1 hr at 37°C in 95% O_2/5% CO_2, washed 7 times with saline, lysed by scraping and sonication, and transferred to a NMR tube for CEST. The lysate of EuL-loaded HeLa cells displayed an obvious CEST signal at 50 ppm with similar features as seen previously for EuL in aqueous buffer (Figure 2B). The amount of EuL per cell as measured by inductively coupled plasma - optical emission spectroscopy (ICP-OES) was $7.5 \pm 1.6 \times 10^{-14}$ mol. If one assumes a cell volume of ~4.2×10^3 μm^3, the intracellular concentration of EuL could be estimated at ~17 mM. This indicates that EuL is highly cell permeable and likely distributes into cells by pinocytosis or macropinocytosis[24] although given the high concentration of agent presented to cells, passive transport could also be partially involved.

Given that $^1O_2$ is widely regarded as the primary effector of tissue damage during PDT,[6,7] quantification of singlet oxygen during treatment may be important for proper dosimetry.[25] The intent of the present work is to investigate whether $^1O_2$ generated upon irradiation of a sensitizer deposited in living cells can simulate PDT *in vitro*. To test this, HeLa cells cultured in a 75 cm^3 culture flask were co-loaded with 15 mM EuL and 2 mM TMPyP and the flask was irradiated from a distance of 10 cm using a 150W tungsten lamp for 30 min. Longer irradiation times were not possible due to cell heating. After irradiation, the cells were washed 7 times, lysed by scraping and sonication, and analyzed by CEST spectroscopy. No significant difference could be detected between the CEST signals (Fig. 2B) of EuL in irradiated *versus* non-irradiated cells. This indicates that the amount of EP-EuL produced during this 30 min period of irradiation was too small to detect by CEST spectroscopy. TMPyP has been reported to localize largely in the nucleus[14] while EuL appears to be localized largely in cytoplasm so any $^1O_2$ produced by TMPyP in this

experiment was likely quenched by water and intracellular $^1O_2$ scavengers (histidine and tryptophan)[26] such that only a few $^1O_2$ molecules may have come in direct contact with EuL. For increased conversion of the intracellular probe to endoperoxide, a more efficient photosensitizer and longer irradiation times may be necessary. Nevertheless, the data suggest that EuL is taken up by cells so may prove useful for monitoring production of intracellular $^1O_2$ during prolonged PDT treatment.

Finally, to demonstrate that this chemical reaction can be imaged by MRI, CEST images of a phantom prepared from four EuL samples exposed to different concentrations of $^1O_2$ (plus a control sample lacking EuL and the lysate of EuL-deposited HeLa cells) were collected by using two different presaturation frequencies, 54 and 47 ppm. The ratio of the water intensity in these two images defines the CEST image. As shown in the images of Figure 3, the samples containing either water alone (sample labeled W) or the lysate of EuL-deposited HeLa cells (sample labeled E) showed no CEST signal while the CEST ratio in images of the remaining four samples varied from 0.48 (10 mM EuL without exposure to $^1O_2$) to 2.34 (10 mM EuL exposed to 30 mM $^1O_2$). This shows that CEST imaging can be used to quantify $^1O_2$ as long as the concentration of EuL is sufficiently high to generate a CEST signal. The concentration of europium in sample E was later found to be only 0.54 mM, well below the CEST detection limit.

In conclusion, we have demonstrated the potential of a europium(III)-based PARACEST probe for detection of singlet oxygen ($^1O_2$) by ratiometric CEST imaging. The probe has several favorable features including high chemical specificity for $^1O_2$, kinetic and thermodynamic stability, rapid reaction kinetics with $^1O_2$, water solubility and a signal that is independent of pH over the physiological range. These combined features indicate that EuL could be useful for MRI detection of $^1O_2$ in many chemical and biological environments. The major limitation of this probe currently is the amount needed for detection by CEST imaging. There are multiple approaches ond might take to improve the sensitivity of this reagent. First, one could replace the carboxyl groups on the glycine substituents with phosphonate ester groups to lengthen the bound water lifetime and thereby increase CEST sensitivity.[27] Second, one could replace the anthracene group on EuL with 10-methyl-9-anthracene, a derivative has been shown to react ~10-fold faster[14] with $^1O_2$. Such replacement should allow greater accumulation of the corresponding EP-EuL endoperoxide derivative over any given period of time and hence improve the prospects of detecting the end-product. A third approach would be to generate low molecular weight polymer[28] of EuL which could result in greater cell uptake of the agent. Finally, newer pulse sequences such as FLEX[29] that do not require RF pre-saturation of the bound water signal may ultimately provide a mechanism to enhance the sensitivity of PARACEST agents such as this. Given these potential enhancements, the probe platform reported here may ultimately prove useful for detection of $^1O_2$ generated in cells during photodynamic therapy.

Supplementary Material

Refer to Web version on PubMed Central for supplementary material.

Acknowledgments

The authors acknowledge partial financial support for this work from the National Institutes of Health (CA-115531, EB-02584, and EB-00482) and the Robert A. Welch Foundation (AT-584).

References

1. Klotz LO, Briviba K, Sies H. Methods Enzymol. 2000; 319:130–143. [PubMed: 10907506]

2. Nishinaka Y, Arai T, Adachi S, Takaori-Kondo A, Yamashita K. Biochem Biophys Res Commun. 2011; 413:75–79. [PubMed: 21871447]
3. Stief TW. Med Hypotheses. 2003; 60:567–572. [PubMed: 12615524]
4. Davies M. J Biochem Biophys Res Commun. 2003; 305:761–770.
5. Langie SAS, Cameron KM, Waldron KJ, Fletcher KPR, von Zglinicki T, Mathers JC. Mutagenesis. 2011; 26:461–471. [PubMed: 21355044]
6. Weishaupt KR, Gomer CJ, Dougherty TJ. Cancer Res. 1976; 36:2326–2329. [PubMed: 1277137]
7. Bonnett R. Chem Soc Rev. 1995; 24:19–33.
8. Kuimova MK, Yahioglu G, Ogilby PR. J Am Chem Soc. 2009; 131:332–340. [PubMed: 19128181]
9. Niedre M, Patterson MS, Wilson BC. Photochem Photobiol. 2002; 75:382–391. [PubMed: 12003128]
10. Schweitzer C, Schmidt R. Chem Rev. 2003; 103:1685–1757. [PubMed: 12744692]
11. Jung MY, Choi DS. J Agric Food Chem. 2010; 58:11888–11895. [PubMed: 21038912]
12. Steinbeck MJ, Khan AU, Karnovsky MJ. J Biol Chem. 1992; 267:13425–13433. [PubMed: 1320020]
13. Tanaka K, Miura T, Umezawa N, Urano Y, Kikuchi K, Higuchi T, Nagano T. J Am Chem Soc. 2001; 123:2530–2536. [PubMed: 11456921]
14. Song B, Wang GL, Tan MQ, Yuan JL. J Am Chem Soc. 2006; 128:13442–13450. [PubMed: 17031957]
15. Li XH, Zhang GX, Ma HM, Zhang DQ, Li J, Zhu DB. J Am Chem Soc. 2004; 126:11543–11548. [PubMed: 15366900]
16. Ward KM, Aletras AH, Balaban RS. J Magn Reson. 2000; 143:79–87. [PubMed: 10698648]
17. Viswanathan S, Kovacs Z, Green KN, Ratnakar SJ, Sherry AD. Chem Rev. 2010; 110:2960–3018. [PubMed: 20397688]
18. Ratnakar SJ, Woods M, Lubag AJM, Kovacs Z, Sherry AD. J Am Chem Soc. 2008; 130:6–7. [PubMed: 18067296]
19. Liu G, Li Y, Pagel MD. Magn Reson Med. 2007; 58:1249–1256. [PubMed: 18046705]
20. Aubry JM, Cazin B. Inorg Chem. 1988; 27:2013–2014.
21. Zhang SR, Winter P, Wu KC, Sherry AD. J Am Chem Soc. 2001; 123:1517–1518. [PubMed: 11456734]
22. Woessner DE, Zhang SR, Merritt ME, Sherry AD. Magn Reson Med. 2005; 53:790–799. [PubMed: 15799055]
23. Werts MHV, Verhoeven JW, Hofstraat JW. J Chem Soc -Perkin Trans. 2000; 2:433–439.
24. New EJ, Congreve A, Parker D. Chem Sci. 2010; 1:111–118.
25. Jarvi MT, Niedre MJ, Patterson MS, Wilson BC. Photochem Photobiol. 2011; 87:223–234. [PubMed: 21143603]
26. Wei CY, Song B, Yuan JL, Feng ZC, Jia GQ, Li C. J Photochem Photobiol A-Chem. 2007; 189:39–45.
27. Rojas-Quijano FA, Benyó ET, Tircsó G, Kálmán FK, Baranyai Z, Aime S, Sherry AD, Kovács Z. Chem Eur J. 2009; 15:13188–13200. [PubMed: 19882595]
28. Wu YK, Zhou YF, Ouari O, Woods M, Zhao PY, Soesbe TC, Kiefer GE, Sherry AD. J Am Chem Soc. 2008; 130:13854–13855. [PubMed: 18817395]
29. Lin CY, Yadav NN, Friedman JI, Ratnakar J, Sherry AD, van Zijl PCM. Magn Reson Med. 2012; 67:906–911. [PubMed: 22287162]

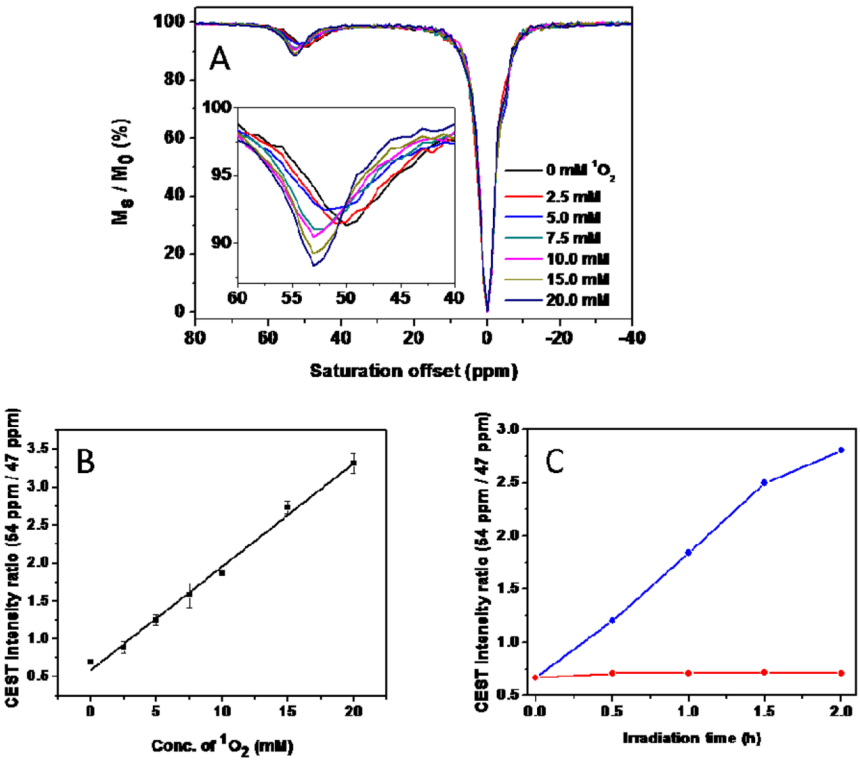

Figure 1.

(A) CEST spectra of EuL before and after reaction with various concentrations of $^1O_2$ generated from MoO_4^{2-}/H_2O_2 recorded at 9.4T and 298 K. Insert: enlarged partial view of the CEST spectra. $[Eu^{3+}]$ = 5 mM, B_1 = 9.4 μT, and sat. time = 4 s. (B) Calibration curve for $^1O_2$ detection derived from the ratio of water intensities after presaturation at 54 *vs* 47 ppm. (C) The changes observed in the CEST intensity ratio (54/47) for samples of 5 mM EuL irradiated in the presence (blue) or absence (red) of 1 mM TMPyP.

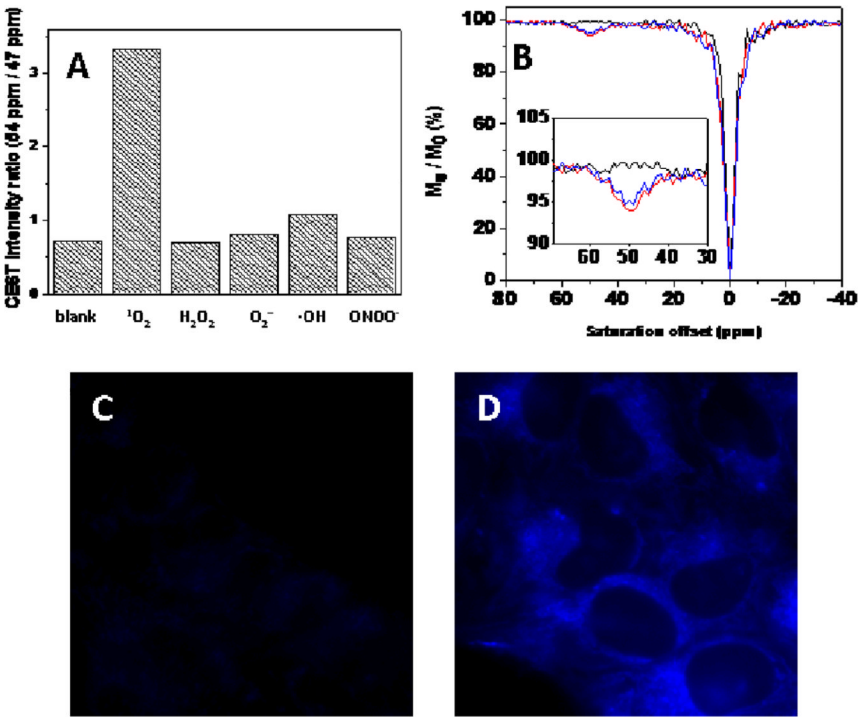

Figure 2.

(A) Comparisons of CEST ratios (54/47) for 5 mM EuL after reaction with different reactive oxygen species: $^1O_2$ (produced by reacting 40 mM H_2O_2 with 50 mM Na_2MoO_4); H_2O_2 (40 mM H_2O_2); •OH (produced by reacting 40 mM H_2O_2 with 40 mM $FeCl_2$); $O_2^{-\bullet}$ (40 mM KO_2); $ONOO^-$ (40 mM NaONOO). (B) CEST spectra of the lysate of HeLa cells incubated in EuL-free saline (black line), loaded with 15 mM EuL (red line) or co-loaded with 15 mM EuL and 2 mM TMPyP, then irradiated by a 150W tungsten lamp (blue line). Insert: enlarged partial view of the CEST spectra. Fluorescence images of HeLa cells incubated without (C) or with 5 mM EuL (D) in physiological saline for 1 hr at 37°C (Objective: Plan-fluor 63×; excitation filter: 350 ± 50 nm bandpass; emission filter: 460 nm ± 50 nm bandpass; exposure time: 0.5s).

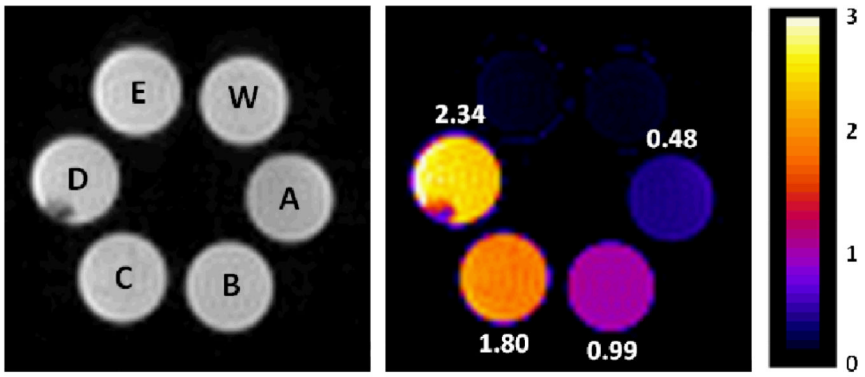

Figure 3.

Images of phantoms containing water alone (W), 10 mM EuL exposed to different concentrations of singlet oxygen (A: 0 mM $^1O_2$, B: 10 mM $^1O_2$, C: 20 mM $^1O_2$, D: 30 mM $^1O_2$) or E: a cell lysate derived from EuL-deposited HeLa cells. The images were recorded at 9.4T and 298 K. (a) Proton density images, (b) ratiometric CEST images after activation at 55 versus 48 ppm.

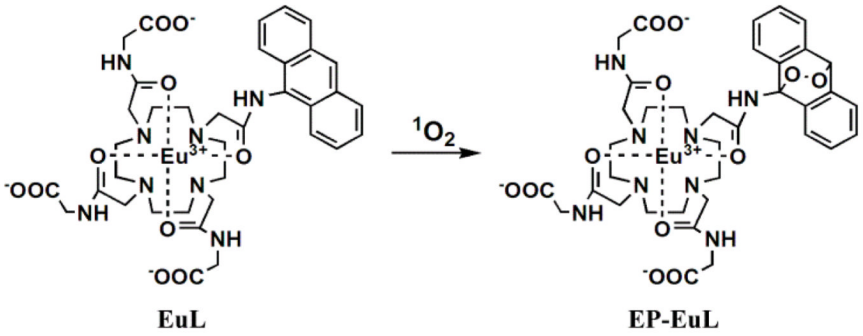

Scheme 1.
Reaction of EuL with $^1O_2$.